Experimental Optics

Contact person:
Roland Ackermann
Friedrich-Schiller-Universität Jena
Abbe School of Photonics
Max-Wien-Platz 1
07743 Jena, Germany
Phone: +49 3641 9-47821, e-mail : Roland.Ackermann@uni-jena.de

Last edition: Roland Ackermann, February 2015

Lab Title: Fundamentals

Group number	G 14
Student name(s)	Ke Li, Jerome Jahn
Name of TA	Maxime Chambonneau and Kim Lammers
Date of Lab	January 18, 2019
Date of Final Report return	

Fundamental Optical Experiments Lab Report

Ke Li , Jerome Jahn

January 2019

Contents

1 Introduction

Light is one of the most important driving forces of the 21st century's technology. To understand how to control light, it is important to understand the behavior of light under different circumstances.

The aim of this set of experiments was to make measurements concerning the fundamental phenomena of light, including the law of reflection and refraction for different media, total internal reflection, dispersion in a prism, diffraction after a grating, and the rotation of light's polarization by birefringent crystals.

2 Theory

2.1 Waves in Optics

2.1.1 General Wave Equation

A travelling wave can be thought of as a diffusing oscillation, or a periodically repeating motion that spreads out in space. Mathematically, a wave function is a solution to the second-order linear partial differential equation shown in equation 1 called the wave equation

$$\nabla^2 f - k^2 \frac{df}{dt^2} = 0. \tag{1}$$

Solutions to the wave equation are typically given as either the sinusoidally varying function in equation 2

$$f(\vec{r}, t) = A\cos(\vec{k} \cdot \vec{r} - \omega t), \tag{2}$$

or the complex exponential function in equation 3

$$f(\vec{r}, t) = Ae^{i(\vec{k}\cdot\vec{r} - \omega t)}. \tag{3}$$

In the above equations, A defines the maximum and minimum value of the wave function and is called the amplitude, k gives the number of radians per unit distance and is called the angular wave number, and ω is the number of radians per unit time and is the angular frequency. Other parameters that may be used are the spatial period, called the wavelength λ, the number of cycles per unit of time, called the temporal frequency f, and the units of distance per unit of time with which a point on the wave moves, called the phase speed or wave speed v. An important equation is the relationship between these three latter variables in equation 4

$$v = \lambda f. \tag{4}$$

For completeness, it is important to mention that the operators in the wave equation are linear. This implies that any sum of solutions is also a solution. Coupled with the Fourier Theorem, which states that any periodic function can be written as a sum of sines and cosines, this implies that any periodically varying amplitude is a solution to the wave equation. These more complex

solutions are required in the study of polychromatic light. However, in the experiments that follow, the light used is assumed to be monochromatic, and can be described simply by either Equation (2) or (3).

2.1.2 Electromagnetic Waves

Light waves are oscillations in the electromagnetic field with vacuum wavelengths between 100 nanometers and 1 millimeter. The electromagnetic field permeates all space and is the mathematical construct describing the interactions of stationary and moving charges. In electrodynamics, it is typically described by two coupled fields, the electric field $\vec{E}$ with units of N/m and the magnetic field $\vec{B}$ in units of Teslas. Maxwell's Equations completely describe these interactions. Any function seeking to describe light needs to satisfy not only the general wave equation but also the macroscopic Maxwell's Equations shown in the set of equations 5

$$\begin{aligned} \nabla \cdot \vec{D} &= \rho \\ \nabla \cdot \vec{B} &= 0 \\ \nabla \times \vec{E} &= -\frac{\delta B}{\delta t} \\ \nabla \times \vec{H} &= \vec{J} + \frac{\delta D}{\delta t}. \end{aligned} \tag{5}$$

The quantities $\vec{D}$ and $\vec{H}$ are interpreted as the total electric field and magnetic field, respectively, within the medium in which the light is propagating. The fact that all wave functions seeking to represent light need to satisfy Maxwell's Equations results in equations between general wave parameters and the physical parameters introduced in electrodynamics. While it is extremely fruitful to consider all of these interrelationships, for an understanding of the nature of reflection, refraction, total internal reflection, diffraction and dispersion, only the concepts of refractive index, the optical path length, and Fermat's Principle of Least Time are required.

As seen in Equation 6, the refractive index n is defined as the ratio of the light wave's wave speed within the medium v to its speed in a vacuum c

$$n = \frac{c}{v} \Longleftrightarrow v = \frac{c}{n}. \tag{6}$$

As the laser sources used have very small powers, less than 5 mW, the radiation pressure of the incident light is not enough to accelerate any surfaces involved in the experiments any appreciable amount. Hence, the assumption will be made that all material boundaries will remain absolutely stationary, and thus the temporal frequency of light will remain constant as light crosses any material boundaries in any experiment. From Equation 6 it follows that in a separate medium, as the wave speed changes so does the wavelength as in Equation 7

$$\frac{c}{n} = \frac{\lambda}{n} f. \tag{7}$$

The optical path length within a medium is defined as the distance light would have travelled in a vacuum in order to have undergone the same amount of phase cycles as it did in a stretch in the medium. It is calculated by multiplying the distance travelled s by the refractive index of the material n as in Equation 8

$$OPL = ns. \tag{8}$$

If there are multiple materials, or the refractive index is a function of the position, the optical path length turns from a product into the sum of products shown in equation 9

$$OPL = \int_a^b nds. \tag{9}$$

Coupled with the laws of classical physics of energy and momentum conservation, the effects observed in this laboratory can be described. The following sections will explore some of these effects.

2.2 Fresnel's Equations

The Fresnel Equations govern the phenomena of reflection and refraction that arise when light hits a surface that acts as a boundary between two spatial regions with different refractive indices. This situation is shown in Figure 1.

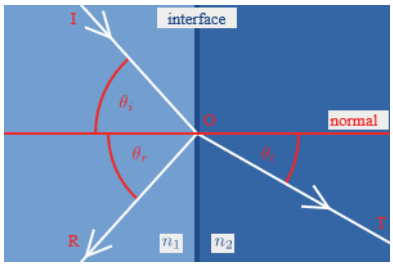

Figure 1: Reflection and Refraction of Light at a Material Boundary

Upon hitting the boundary, some of the incident light bounces off and is reflected, whereas the other part passes into the other material with a change in direction that depends nonlinearly on the ratio of the refractive indices. The law of reflection governs the interaction of light with a reflective material. As Figure 2 (3) shows, the law of reflection states that the incident angle i equals to the reflected angle r. Both angles are measured with respect to the normal plane to the interface.

$$i = r \tag{10}$$

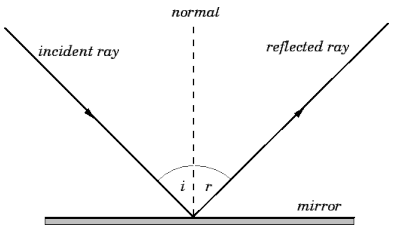

Figure 2: The Law of Reflection

When a ray of light travels from one medium to another, the ray will change its direction of propagation. This phenomenon is called refraction. The mathematical form of refraction is given by Snell's law in equation 11

$$\frac{\sin\alpha}{\sin\beta} = \frac{n_\beta}{n_\alpha}, \tag{11}$$

where α is the incident angle of light from the medium with refractive index n_α with respect to the plane normal to the surface of the interface of the two media, and β is the refracted angle of light in the second medium with the refractive index of n_β with respect to the plane normal to the interface of the two media.

2.3 Parallel Shift

When light travels through a parallel plate of opaque medium with different refractive index $n_r(w)$, the output light is shifted with distance d away from the path of the incident light. As Figure 3 shows, the phenomenon occurs when light is refracted twice, one when entering the medium, and the other time when exiting the medium.

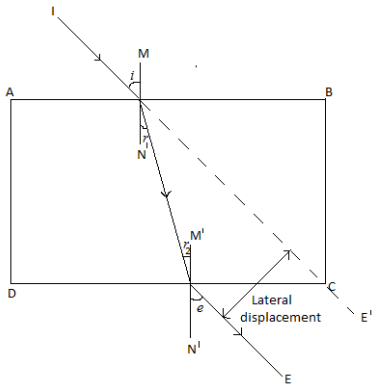

Figure 3: Parallel Shift

Due to the symmetric structure of the parallel plate, the first refraction angle r_1 equals to the second refraction angle r_2 ($r_1 = r_2$). The perpendicular distance between the direction of the incident ray and the output ray is called lateral shift. The lateral shift distance (d) can be calculated with equation 12

$$d = b\frac{\sin(i-r)}{\cos(r)}, \tag{12}$$

where i is the incident angle with respect to the plane normal to the interface, r is the refracted angle with respect to the plane normal to the interface, and b is the width of the parallel plate.

2.4 Total Internal Reflection

When light travels from a medium with lower refractive index to a medium with higher refractive index, it is observed that there is a maximum angle for which a refracted light beam will occur in the medium with higher refractive index. At the maximum angle, the angle of the refracted light is 90°from the normal. The incident angle of the light when this occurs is called "critical angle". The incident angle being larger than the critical angle will cause a phenomenon called "total internal reflection". Figure 4 shows an example of total internal reflection for a water-air interface.

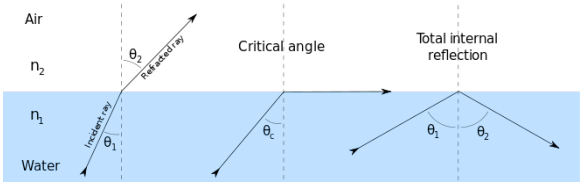

Figure 4: Total Internal Reflection

The critical angle is calculated using Snell's Law of Refraction (Equation 11) in the form shown in Equation 13 below

$$\sin\theta_2 = \frac{n_{\theta 2}}{n_{\theta 1}}\sin\theta_1. \tag{13}$$

Here n_2 is the refractive index of the denser medium, n_1 is the refractive index of the less dense medium, θ_1 the refracted angle in the less dense medium, and θ_2 the incident angle from the denser medium. Setting $\theta_1 = 90°$ gives the expression for the critical angle shown in Equation 14 below

$$\theta_c = \arcsin\frac{n_{\theta 2}}{n_{\theta 1}}. \tag{14}$$

2.5 Beam Propagation through Prism

When light travels through a prism, reflection and refraction will happen at each surface that the light strikes, unless it hits a prism-air boundary at an

angle from the normal that is greater than the critical angle. In this latter case, the light will be totally internally reflected. These two situations are shown in Figure 5 below.

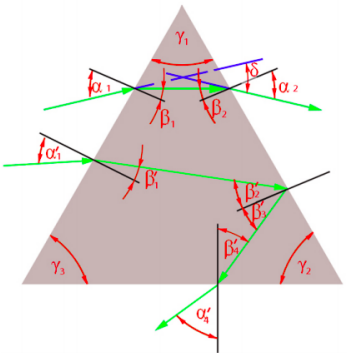

Figure 5: Beam Propagation Through Prism

Due to different incident angle of the light, total internal reflection might happen on the second side of the beam. The total refraction angle δ could be calculated from the equations 15- 20 (4)

$$\delta = (\alpha_1 + \alpha_2) - (\beta_1 + \beta_2) \tag{15}$$

$$\sin\beta_1 = \frac{n_\alpha}{n_\beta}\sin\alpha_1 \tag{16}$$

$$\delta = (\alpha_1 + \alpha_2) - \gamma_1 \tag{17}$$

$$\beta_2 = \gamma_1 - \beta_1 \tag{18}$$

$$\gamma_1 = \beta_1 + \beta_2 \tag{19}$$

$$\sin\alpha_2 = \frac{n_\beta}{n_\alpha}\sin\beta_2. \tag{20}$$

As can be seen in Figure 4, if the incident angle α_1 is smaller than the output angle α_2, the total internal reflection will occur on the base of the prism.

The special case where the light travels parallel to the base of the prism is shown in Figure 5. In this case, the angle of deviation from the input light is minimum. Considering the geometry of the prism, the value of this minimum angle between the transmitted and incident beams $\alpha_m in$ can be calculated using equation 21 below

$$\alpha_m in = 2(\alpha_1 - (90^\circ - \gamma)), \tag{21}$$

where $alpha_1$ is the incident angle from the normal and γ is the prism angle. The minimum angle of deviation can be used to calculate the refractive index of the prism with equation 22

$$n_\beta(\lambda) = \frac{\sin\left(\frac{\alpha_{min}}{2} + \frac{\gamma}{2}\right)}{\sin\left(\frac{\gamma}{2}\right)}, \tag{22}$$

where the refractive index in the prism is frequency-dependent. α_{min} is the deviation angle between the incident and the transmitted beam, which occurs when the light is travelling parallel to the prism's base. γ is the prism angle, which in the case of equilateral triangle, equals 60°.

2.6 Prism Dispersion

As introduced in section 2.5, the refractive index of a prism is frequency dependent. Light with different frequencies travels at different speeds inside the prism, resulting in frequency-dependent angles of refraction. As Figure 6(4) shows, red light has a lower refractive index than green light. Green light thus bends more sharply.

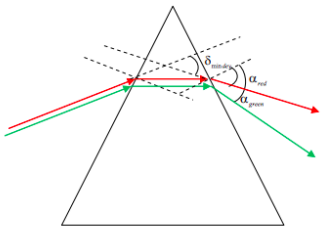

Figure 6: Prism Dispersion

The dispersion in a prism can be quantitatively described by equation 23

$$dispersion \approx \frac{\partial \alpha}{\partial \lambda} \approx \frac{\alpha_{red} - \alpha_{green}}{\lambda_{red} - \lambda_{green}}, \tag{23}$$

where α_{green} and α_{red} are the minimum angles that the refracted beams deviate from the angle of the incident beams. The maximum dispersion occurs when the light travels parallel to the base of the prism.

2.7 Grating Dispersion

Consider a planar light wave traveling in a homogeneous medium incident on a perfectly absorptive wall that has a small, narrow slit in it. The slit width d is on the order of the distance between the wavefronts of the light λ. A screen is placed at a distance L from the slit that is much larger than the width of the slit itself. This situation is depicted in Figure 7 below.

Consider the paths that light can take to reach a point on the screen. Obviously, the starting points of the light need to lie within the width of the slit. By Fermat's Principle of Least Time, the light that originates at any point within

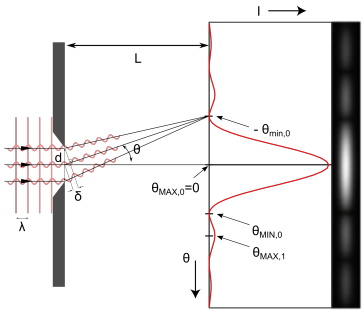

Figure 7: Single-slit Diffraction onto an Image Plane

the slit travels to the screen in a straight line and can thus be thought of as rays. The intensity pattern measured on the screen is then due to the interference of light rays originating from points within the slit.

Calculating the optical path difference between the ray originating at the slit's top edge and the slit's bottom edge to a general point on the screen leads to a simple formula for the vertical position of the intensity maxima on the screen as a function of the inclination from the horizontal θ, the slit width d, and the incident wavelength λ. The intensity maxima are called diffraction orders, with the central maximum being labeled the 0th order, the neighboring diffraction orders being labeled the 1st diffraction orders, and so on. In Figure 7, the 0th order is the brightest maximum, the 1st order is the 2nd brightest maxima, and so on. This intensity relationship between the diffraction orders is typical of the single-slit diffraction phenomenon.

A grating is a material boundary that is essentially only periodically spaced slits with period d separated by an absorptive medium in between. The dispersive character of the grating is shown in Figure 8.

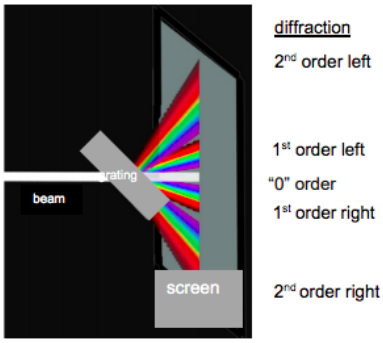

Figure 8: Diffraction after a Grating

The intensity pattern on a screen placed a distance L from the grating is the

result of the interference of light waves from the top and bottom edge of each of the slits. A grating is characterized usually by the number of slits per millimeter on the grating N, with N typically being either 100, 300, or 600 $mm^{-}1$ (4). As in the single-slit diffraction scenario, the spacing between the diffraction orders is a function not only of the grating's slits' width d and the distance from the grating L, but also the wavelength incident onto the grating λ. The formula for the angle from the horizontal Θ at which each wavelength is diffracted is given by Equation 24

$$sin(\Theta) = \frac{k\lambda}{d}, \tag{24}$$

where k is any nonnegative integer and denotes the diffraction order. Due to the dependence of the pattern on the frequency of the incident light, this is a dispersive diffraction effect. The grating dispersion is given by Equation 25 below

$$dispersion = \frac{\delta\alpha}{\delta\lambda} \approx \frac{\delta\alpha_r ed - \delta\alpha_g reen}{\delta\lambda_r ed - \delta\lambda_g reen}. \tag{25}$$

Here, α is the angular position of a diffraction order and λ is the wavelength incident on the grating.

By altering the slits physically by introducing a blaze angle, it is possible to fine-tune this interference pattern so as to direct the vast majority of the light onto a specific diffraction order. This tuning can only be done perfectly for a singular frequency within a homogeneous medium, but even for different frequencies a particular diffraction order can be made brighter than the rest.

2.8 Brewster angle

Light traveling through a vacuum can be thought of as synchronized spreading oscillations in the electric and magnetic fields. The fundamental interaction between these oscillations is described by Maxwell's Equations (Equation 5) in the absence of charge density ρ and current density $\vec{J}$. These oscillations are perpendicular to each other and to the direction of propagation of the light, as shown in Figure 9 below.

Figure 9: A Linearly Polarized Light Wave Traveling in a Vacuum

It is important to note that this situation is only exactly true for light traveling in a perfect vacuum. In general, when light is traveling within a medium,

there is a component of the electric and magnetic fields that points along the axis of propagation as well. With the refractive index of air being so close to a vacuum however, the longitudinal aspect of the electromagnetic wave will be assumed to be zero.

When visible light wavelengths are incident on a dielectric such as plastic or glass, the bound electrons at the surface of the material will interact with the light. The electromagnetic wave will move these electrons from their preferred positions and make each atom an electric dipole. The sum of the dipole fields is called the polarization field of the material. When the materials are nonmagnetic, the interaction of the magnetic field vector with the material's atoms can be neglected.

In considering the incident electric field's effect on the atoms on the surface of the material, the important components of $\vec{E}$ are the component parallel to the surface $\vec{E_{\parallel}}$ and component perpendicular to the surface $\vec{E_{\perp}}$. These will by definition by orthogonal and are not coupled.

In general, both components of the incident light will be reflected and transmitted. However, there is an incident angle called the Brewster angle where $\vec{E_{\perp}}$ is fully transmitted. The reflected light will consist of purely a portion of $\vec{E_{\parallel}}$. At the Brewster angle, the reflected and refracted light have a 90° angle between them. The reflection and refraction of light incident at the Brewster angle is depicted in Figure 10.

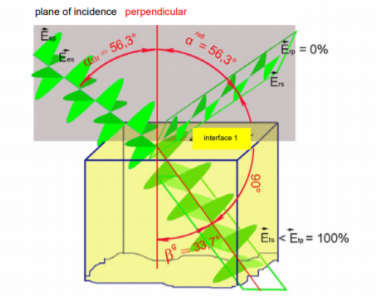

Figure 10: The Reflection and Refraction of Light Incident on a Dielectric

The expression for the Brewster angle follows from Snell's Law of Reflection and Refraction and the condition that the angle between the rays is 90°. The result is Equation 26.

$$\tan(\alpha_{Br}) = \frac{n_2}{n_1}. \tag{26}$$

2.9 Birefringence and Optical Activity

Birefringence is a material property of materials with molecular ordering. Light propagating along the optical axis, or the axis around which the material has rotational symmetry, experiences a different refractive index as light propagating

in other directions. Essentially, the part of the light that is polarized to oscillate perpendicular to the optical axis will experience the ordinary refractive index, whereas the rest of the light without this component will experience an angle-dependent extraordinary refractive index. The relationship of these indices on the propagation direction is shown in Figure 11.

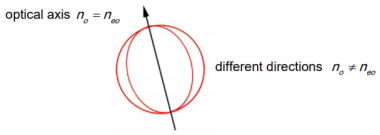

Figure 11: Birefringence in a Single-Axis Crystal

For materials with multiple optical axes, there would be a different refractive index diagram. In this set of experiments, a uniaxial crystal was used. The effect of birefringence is to rotate the polarization of light. The ordinary and extraordinary components of the light have different optical path lengths through the crystal, which causes varying phase differences as a function of the propagation distance through the crystal. When light goes from crystal to air, these phase differences in the vectorial amplitudes of the ordinary and extraordinary ray cause a new polarization that will have been rotated from the polarization with which the light was incident onto the crystal.

3 Experimental Setup

3.1 Basic Experiment Setup and Description

The experimental setup in general consisted of a base holding the laser, supplementary materials such as blocks and mounts to be placed on top of and in front of the base, and a set of measurement templates which facilitated the alignment of the setup and the taking of data. The setup is shown in Figure 12 (4).

The base was transparent and sported a track in which a movable mount with a laser source was attached. The track allowed for the positioning of the laser along a circular arc. The base was placed on top of the measurement templates used in each experiment. Each measurement template had a protractor drawn on it that allowed for the measurement of the angle that the laser light made with the normal. There were a variety of other markings on each measurement template, including other protractors and shaded outlines that were labeled with the supplementary material that was to be placed within the outline. The transparent base had notches against which the various faces of the supplementary materials could be pressed to ensure their alignment with the measurement template. Each of the following sections had their own measurement template.

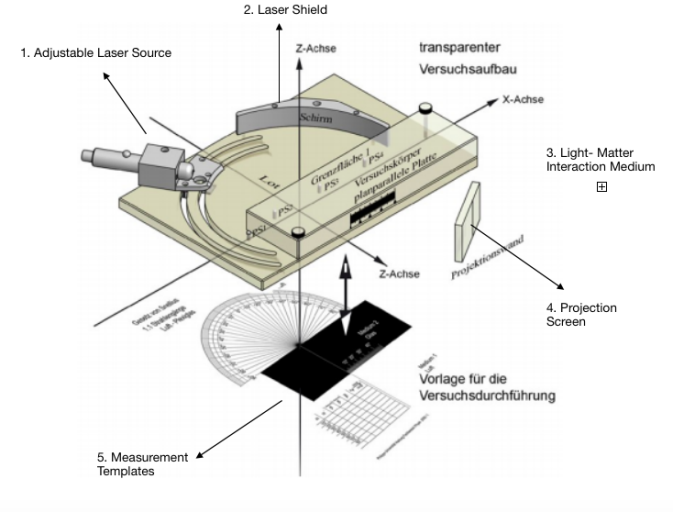

Figure 12: General Experiment Setup

3.2 Beam Propagation, Law of Reflection, and Snellius Law Experiment

3.2.1 Air-Metal and Air-Plexiglas Transition

a) Air-Metal: Law of Reflection Experiment

To examine the reflection law for metal, a simple measurement template with only a 180° protractor was used.

After placing metal on the sample location, the angle of laser source was adjusted so that the input angle from the normal ranged from 20° to 70° with 10° steps. At each step, the reflection angle α from the normal was measured.

b) Air-Plexiglas : Law of Reflection and Refraction

The Plexiglas was placed on the sample location on the measurement template shown in Figure 13 below.

The laser source adjusted to an angle from the normal of 20° to 70° with 10° steps. The reflection angle $\alpha^{'}$ and refraction angle β was measured at each step.

3.2.2 Air-Water

A box of clean water with thin transparent sides was placed on the sample location on the measurement template shown in Figure 14 below.

The laser source was adjusted so that the input angle of the laser beam to the water was at $15°, 20°, 25°, 30°$ and $40°$. The refracted angle γ_{water} was recorded for each input angle.

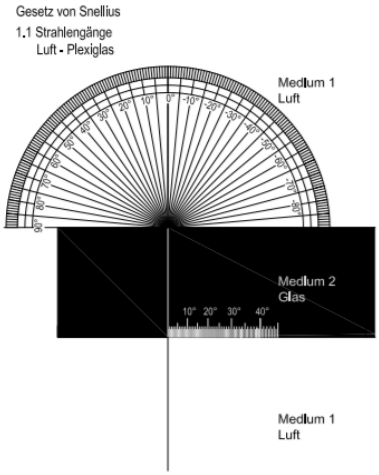

Figure 13: Measurement Template for Air-Plexiglas Reflection and Refraction

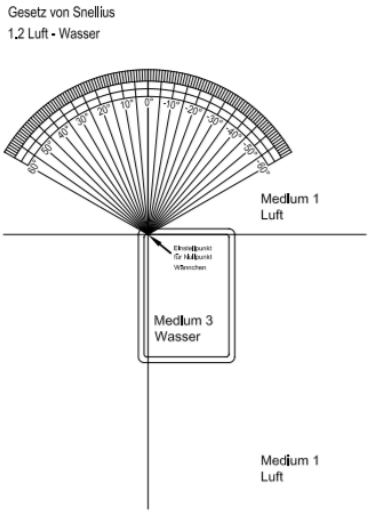

Figure 14: Measurement Template for Air-Water Reflection and Refraction

3.2.3 Plexiglas-Water

Both a water sample and Plexiglas sample were placed at their respective sample location on the measurement template shown in Figure 15 below.

The laser sources were adjusted so that the laser light pointed into the Plexiglas at the angle $\beta : 10°, 15°, 20°, 25°$. The refracted angle from glass to water γ_{water} was measured at each angle.

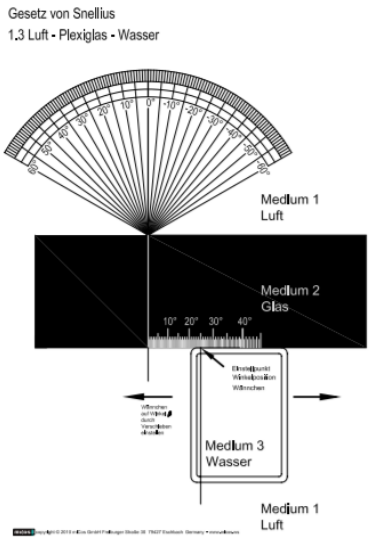

Figure 15: Measurement Template for Plexiglas-Water Reflection and Refraction

3.2.4 Parallel Shift

In order to measure the parallel shift of the incident light passing through the Plexiglas, we used the measurement template shown in Figure 16 below.

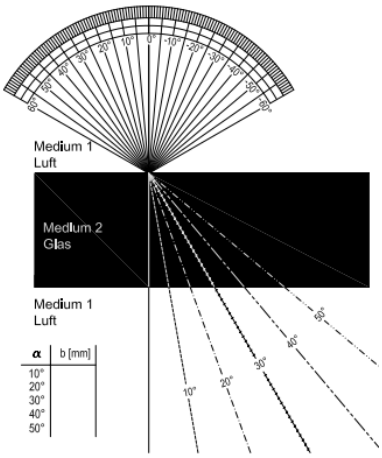

Figure 16: Parallel Shift Template

The parallel shift of the light beam (d mm) was measured for incident angle of $\alpha = 20°, 30°, 40°, 50°$ respectively. We took the measured refractive angle

for Plexiglas $\beta_{measured}$ for these angles, and recorded the respective value of parallel shift for these angles by placing our measurement ruler perpendicular to the angle measurement line and the output beam shown in Figure 8. Because our measurement ruler is made out of a Plexiglas and produced the same parallel shift effect when we measured d, we only recorded the experiment data where the measurement is taken on the measurement lines shown in Figure 16.

3.2.5 Total Internal Reflection with Plexiglas Plate

To examine the phenomenon of total internal reflection in a Plexiglas plate, the measurement template shown in Figure 17 below was used.

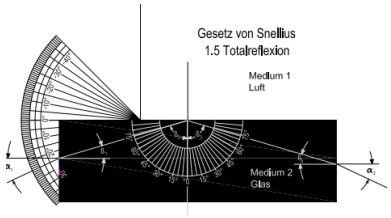

Figure 17: Total Internal Reflection with Plexiglas Plate Measurement Template

The incident angle of the light α_1 was adjusted until total internal reflection of the light at the upper Plexiglas-air boundary was observed.

3.2.6 Total Internal Reflection with Plexiglas Arc Forms

To examine the phenomenon of total internal reflection, when light travels from a high refractive index medium to low refractive index medium, we used the experiment setup as shown in Figure 18 below.

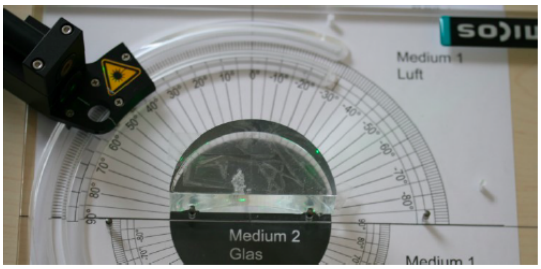

Figure 18: Parallel Shift Template

We moved the adjustable laser source to an angle and observed the refraction of the laser beam. We recorded the angle when we observed that no refracted light is coming out of the flat side of the Arced Plexiglas and the laser beam is completely reflected within the Plexiglas.

3.2.7 Semicircular Plexiglas Brewster Angle Measurement

To measure the Brewster angle of the semicircular Plexiglas form, the measurement template shown in Figure 19 was used.

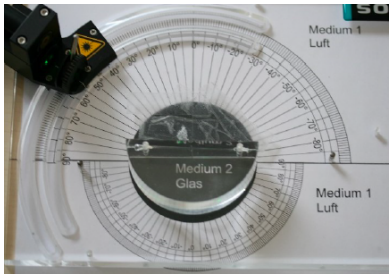

Figure 19: Brewster Angle Measurement Setup

A polarizer was placed in front of the laser source. The laser position and polarizer were simultaneously adjusted until there was no reflected beam.

3.3 Propagation through Prism and Prism Dispersion

To measure the reflection and refraction of light in a prism, the measurement template shown in Figure 20 below was used.

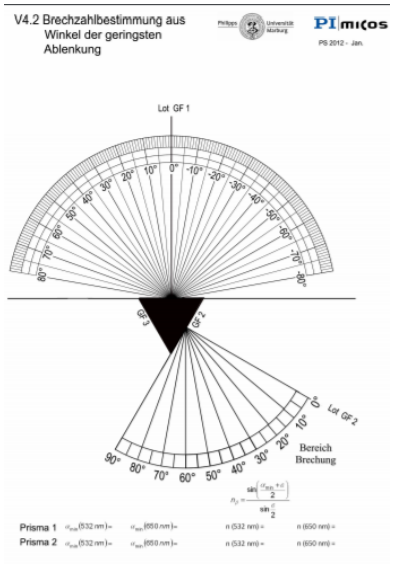

Figure 20: Measurement Template for Prism Experiments

A triangular prism was placed in the shaded outline of the measurement template. The green laser was then aimed at it from angles to the normal of

$10°, 20°, 40°$, and $50°$. The reflected and refracted beams within the prism were observed and recorded.

The green laser was then aimed at the prism so as to run through the prism in a direction parallel to the prism's base. This was determined by checking with a slip of paper whether the entrance and exit locations of the laser were two points that were on a line parallel to the base. The angle for which this occurred was notated. This was repeated with the red laser.

3.4 Diffraction

To measure the positions of the first and second diffraction orders of both the red and the green laser, the measurement template shown in Figure 21 below was used.

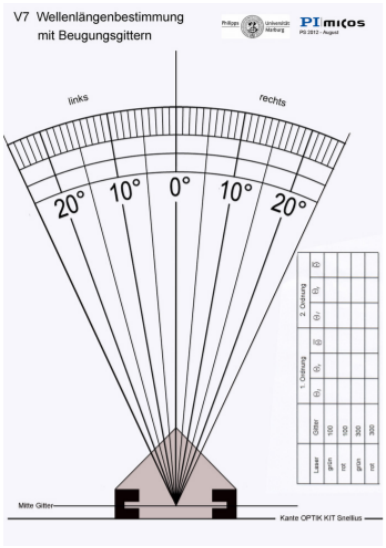

Figure 21: Measurement Template for Measuring Grating Diffraction Orders

First, the green laser was aimed parallel to the normal at the diffraction grating. A sheet of paper was held by hand so as to be a curved screen, such that all diffraction orders would ideally travel the same distance from the grating to the screen. By looking at the diffraction orders from above, the protractor on the measurement template was used to judge the angles at which the diffraction orders were emitted. First, the angular position of the 0th diffraction order was determined. Then the angular positions of the first and second diffraction orders on the left and the right were determined. This was repeated for the red laser.

3.5 Polarization Rotation by Birefringent Crystal

To measure the rotation of the light's polarization by three different birefringent crystals, the measurement template shown in Figure 22 below was used.

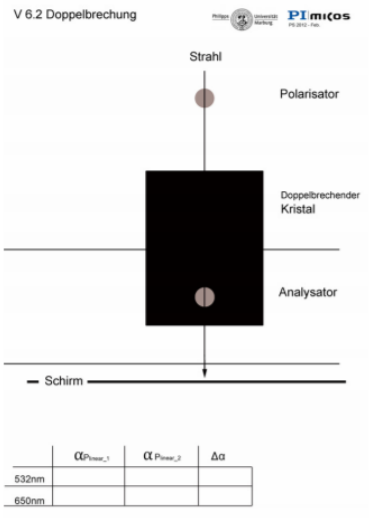

Figure 22: Measurement Template for Birefringence

Two polarizers were inserted into the outlines on the template. They were adjusted until no light could pass through the second polarizer. Their orientation was read from their mounts and notated. Then a birefringent crystal was placed in between them such that the laser light would pass through the crystal. The polarizers were then adjusted again such that no light would be able to pass through the second polarizer. The orientations were again read from their mounts and notated. This was repeated for the three birefringent crystals at the group's disposal.

4 Results

4.1 Beam Propagation, Law of Reflection, and Snellius Law Experiment

4.1.1 Air-Metal and Air-Plexiglas Transition

a) Air-metal reflection The experiment data of law of reflection for the air-metal interface is shown in Table 1. As can be seen from the experiment data, the input angle α equals the reflected angle$\alpha^{'}$. The 0.5° of uncertainty comes from the width of the laser beam and the scale of the protractor.

b) Air-Plexiglas reflection , refraction, and index of refraction

α	$20°$	$30°$	$40°$	$50°$	$60°$	$70°$
$\alpha^{'}$	$20° \pm 0.5°$	$30° \pm 0.5°$	$40° \pm 0.5°$	$50° \pm 0.5°$	$60° \pm 0.5°$	$70° \pm 0.5°$

Table 1: Air-Metal Reflection Experiment Data

The experimental data for air-Plexiglas reflection and refraction is shown in Table 2. Equation 11 was used to calculate the values, with n

$$n_g = n_{air} \frac{\sin \alpha}{\sin \beta}, \tag{27}$$

was used to calculate the refractive index of the Plexiglas. Here n_g is the refractive index of the glass, n_{air} is the refractive index of the air, with a value of 1.0003 taken from literature (5), α the incident angle of the laser beam, and β the refracted angle of the laser beam in the Plexiglas.

α	$20°$	$30°$	$40°$	$50°$	$60°$	$70°$
$\alpha^{'}$	$20 \pm 0.5°$	$30 \pm 0.5°$	$40 \pm 0.5°$	$50 \pm 0.5°$	$60 \pm 0.5°$	$70 \pm 0.5°$
β	$13.5° \pm 0.5°$	$19.5° \pm 0.5°$	$25° \pm 0.5°$	$30° \pm .5°$	$35° \pm 0.5°$	$38.5° \pm 0.5°$
n_g	1.47	1.50	1.52	1.53	1.51	1.51

Table 2: Air-Plexiglas reflection , refraction, and index of refraction Experiment Data

Calculated from the table above, the average value refractive index of the Plexiglas for $532nm$ laser is 1.50.

The deviation of the calculation can be deduced from the equation below:

$$\sigma_n^2 = \frac{\sum_1^6 (\bar{n_{glass}} - n_j)^2}{6} = 0.004. \tag{28}$$

Thus, the final result of the refractive index of the Plexiglas is:

$$n_{glass} = 1.50 \pm 0.02 \tag{29}$$

As shown in Figure 7, the reflected beam $\alpha^{''}$ is observed to be parallel to the reflected beam $\alpha^{'}$. As we can observe in Figure 7, a portion of the input beam(β) is refracted at the first air-Plexiglas interface, and travel inside the Plexiglas. After reaching the second air-Plexiglas interface, a portion of the beam is reflected(beam $\beta^{'}$) and refracted again at the first Plexiglas-air interface, resulting in the parallel refracted beam $\alpha^{''}$ Because $\alpha^{''}$ goes through two times of refraction, it is much dimmer than the input beam α.

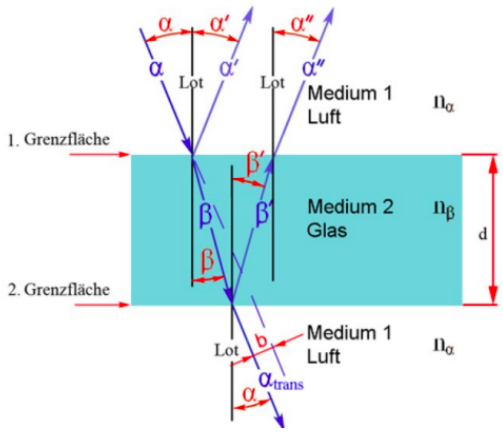

Figure 23: Air-Plexiglas Transition

α	15°	20°	25°	30°	35°	40°
γ	$12.5 \pm 0.5°$	$16.5 \pm 0.5°$	$20 \pm 0.5°$	$23.5 \pm 0.5°$	$26.5 \pm 0.5°$	$30 \pm 0.5°$
n_γ	1.20	1.20	1.24	1.25	1.29	1.29

Table 3: Air Water Refraction Experiment Data

4.1.2 Air-Water

Calculated from the result in Table 3, the average refractive index of water is: 1.24 for the 532 nm green laser. Comparing to the imperial result of 1.33 the refractive index we calculated deviates 7 from the expected values. The deviation of our measurement with similar calculation scheme as equation 28 is: 0.09. Our final measurement result is therefore:

$$n_{gamma} = 1.24 \pm 0.09 \tag{30}$$

4.1.3 Plexiglas-Water

β	10°	15°	20°	25°
γ_{water}	$11.5 \pm 1°$	$17.5 \pm 1°$	$23 \pm 1°$	$28.5 \pm 1°$
$n_{\beta\gamma}$	1.31	1.30	1.32	1.33

Table 4: Plexiglas Water Experiment Data

From the air-Plexiglas experiment, we had the average value of refractive index of Plexiglas $n_{glass} = 1.506nm$. Thus, we can calculate the refractive

index of glass to water transition with the equation:

$$n_{\beta\gamma} = n_{glass}\frac{\sin\beta}{\sin\gamma} = \frac{n_\gamma}{n_\beta} \tag{31}$$

The result is listed in Table 4. The average value of $n_{\beta\gamma}$ calculated from the data is 1.32, the deviation of our measured data is : 0.02. Our final measurement result is therefore:

$$n_{\beta\gamma} = 1.32 \pm 0.02 \tag{32}$$

4.1.4 Parallel Shift

The data collected for calculating the parallel shift of the incident beam of the Plexiglas is listed in table 5. The parallel shift can be calculated with the following equation:

$$b = d \times \frac{\sin\alpha - \beta}{\cos\beta} \tag{33}$$

where b is the parallel shift of the Plexiglas, d is the width of the Plexiglas that the light beam travels through, α the angle of incident, β the corresponding measured refractive angle. In our experiment, $d = 58.5mm$.

α	$20°$	$30°$	$40°$	$50°$
$\beta_{measured}$	$13° \pm 0.5°$	$19.5° \pm 0.5°$	$25° \pm 0.5°$	$30° \pm 0.5°$
$b_{p_measured}(mm)$	7 ± 1	12 ± 1	17 ± 1	23 ± 1
$b_{p_expected}(mm)$	7.316	11.309	16.706	23.103

Table 5: Parallel Shift of the Plexiglas

4.1.5 Total Internal Reflection with Plexiglas Plate

Figure 8 is the measurement template that we used to measure the critical angle and total internal reflection angle in this experiment. We measured an $\alpha_1 = 25°$. As we know theoretically that, when light projects from a medium with higher refractive index to a medium with lower refractive index, total internal reflection occurs. We know that due to the law of reflection, $\alpha_1 = \alpha_2$, where α_1 is the incident angle and α_2 is the output angle. From test 1.1, we know the refractive index of the Plexiglas, which is $n_{glass} = 1.506$, thus, when $\alpha_1 = 25°$, $\beta_1 = \beta_4 = 16.297°$. From trigonometric identities, and the law of reflection, we obtained that: $\beta_2 = \beta_3 = 90° - \beta_1 = 73.703°$.

4.1.6 Total Internal Reflection with Semicircular Plexiglas Form

The averaged critical angle we measured for Plexiglas in arc form for green laser is: $\alpha_{critical} = 43.0° \pm 0.5°$.

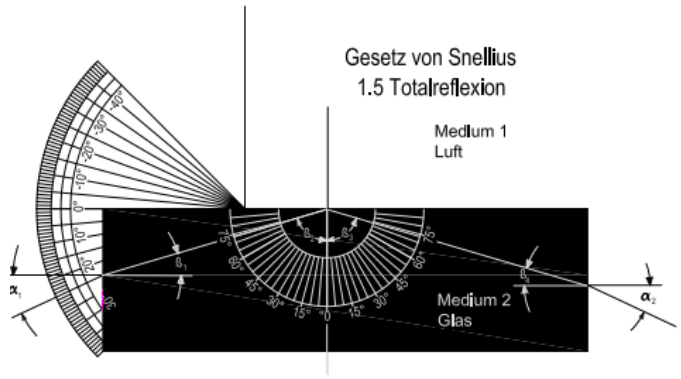

Figure 24: Total Internal Reflection Measurement Template

From equation 12) we can calculate the refractive index of Plexiglas: $n_{glass} = 1.4663$, which is close to the value we obtained in test 1.1 , where $n_{glass} = 1.506$.

4.1.7 Brewster Angle Measurement with Plexiglas Semi Arc Forms

The Brewster angle we measured from the experiment for the semicircular Plexiglas is: $\alpha_{Brew} = 57° \pm 0.5°$. From the equation:

$$n_{glass} = \frac{1}{\arctan \alpha_{Brew}} \tag{34}$$

we can calculate again the refractive index of the Plexiglas. The refractive index calculated from the Brewster angle of the Plexiglass is thus: 1.2774.

4.2 Propagation through Prism and Prism Dispersion

The group used the green laser to investigate light propagation through a prism. It was observed that when the prism was placed in the shaded outline on the measurement template, there were ranges of incident angles that resulted in similar behavior of the light within the prism. These regions are already marked on the measurement template. The group observed the reflection and refraction and made a qualitative description with rough angle measurements to give an idea of the laser beam's behavior. If the light was incident at roughly 10° - 30° from the normal, it would partially reflect from the top surface, totally reflect from the bottom right surface, then partially reflect from the bottom left surface, totally reflect from the bottom right surface again and refract out of the prism at the top surface. There were two laser spots observed above the top surface, and one laser spot observed left of the bottom left surface. If the light was incident at roughly 30° - 35° from the normal, it would partially reflect from the top surface, partially reflect at the bottom right surface, and then refract out of the prism at the bottom left surface. One laser spot was observed above

the top surface, and one was observed left of the bottom left surface. If the light was incident at roughly 35° - 50° from the normal, it would partially reflect from the top surface, partially reflect from the bottom right surface, partially reflect from the bottom left surface, and then exit the prism through the top surface again. There were two laser spots observed above the top surface, one to the right of the bottom right surface, and one left of the bottom left surface.

The angle of minimum inclination α, or the incident angle at which the laser beam propagates parallel to the base of the prism inside the prism, was found next for the green and red laser. The measurements are provided in Table 6 below. The uncertainty stems from the measurement template's scale and the spot size of the laser beam.

Laser	α
Green	$65.0° \pm .50°$
Red	$50.5° \pm .50°$

Table 6: Incident Laser Angles for Parallel Beam Propagation

The prism dispersion was calculated using equation 22. The group obtained a value of $1.23x10^8 \frac{degrees}{meter} \pm 8.5x10^6 \frac{degrees}{meter}$, where the absolute value of the dispersion was taken at the end.

The angle of minimum deviation for the red and green laser was calculated using equation xx. The prism angle for the equilateral triangular prism was taken to be $\gamma = 60°$. The angles are given in Table 7 below.

The refractive index of the prism as a function of the wavelength was calculated the values in Table 7 using equation 21. The values are presented in Table 8 below.

4.3 Diffraction

The angular positions of the green laser's diffraction orders are written in Table 7 below.

The red laser's diffraction order measurements are in Table 8 below.

The errors in the measurements were due to the large spot size and the difficulty in manually shaping a piece of paper into a curved screen.

Using these values, the grating dispersion was calculated using Equation 24. For each diffraction order, the calculated grating dispersion is given below. The

Laser	α_m
Green	$70° \pm 1°$
Red	$41° \pm 1°$

Table 7: Angles of Minimum Deviation

Laser	Refractive Index
Green (532 nm)	1.532±
Red (650 nm)	1.161±

Table 8: Prism's Refractive Index for Red and Green Laser

Diffraction Order	α
1st (left)	$3.0° \pm .50°$
2nd (left)	$6.5° \pm .50°$
1st (right)	$-3.0° \pm .50°$
2nd (right)	$-7.0° \pm .50°$

Table 9: Green Laser Diffraction Order Angular Positions

Diffraction Order	α
1st (left)	$4.5° \pm .50°$
2nd (left)	$8.5° \pm .50°$
1st (right)	$-4.5° \pm .50°$
2nd (right)	$-8.5° \pm .50°$

Table 10: Red Laser Diffraction Order Angular Positions

absolute value of the difference was taken. The values of the wavelengths λ were 532 nm for the green laser and 650 nm for the red laser.

Diffraction Order	Grating Dispersion
1st (left)	$1.3 \times 10^7 \frac{degrees}{meter} \pm 4.2 \times 10^6 \frac{degrees}{meter}$
2nd (left)	$1.7 \times 10^7 \frac{degrees}{meter} \pm 4.2 \times 10^6 \frac{degrees}{meter}$
1st (right)	$1.3 \times 10^7 \frac{degrees}{meter} \pm 4.2 \times 10^6 \frac{degrees}{meter}$
2nd (right)	$1.3 \times 10^7 \frac{degrees}{meter} \pm 4.2 \times 10^6 \frac{degrees}{meter}$

Table 11: Grating Dispersion Calculated at Each Diffraction Order

4.4 Transmission through Polarizers and Birefringent Crystals

The angles at which the polarizers were set in order to block the light once the birefringent crystal was placed in between them is shown in Table 12 below.

The polarizer angle difference describes the change of the 2nd polarizer from its initial position of $-5° \pm 5°$. The positive and negative values indicate the side from the vertically centered position. When looking at the light's polarization

Birefringent Crystal	1st Polarizer Angle	2nd Polarizer Angle	Polarizer Angle Difference
No Crystal	$40° \pm 5.0°$	$-5° \pm 5.0°$	$50° \pm 10°$
Crystal 1	$40° \pm 5.0°$	$25° \pm 5.0°$	$30° \pm 10°$
Crystal 2	$40° \pm 5.0°$	$55° \pm 5.0°$	$60° \pm 10°$
Crystal L	$40° \pm 5.0°$	$-30° \pm 5.0°$	$-25° \pm 10°$

Table 12: Polarizer Angles and Angle Differences for each Birefringent Crystal

from behind, facing the propagation direction while it moves straight away, positive angle measurements meant that the polarizer was rotated clockwise. Negative angle values indicate that the polarizer was rotated counterclockwise.

The measurements made of the angular displacement of the polarizers determine whether the bifrefringent crystals labeled $1, 2$, and L rotated the light polarization clockwise or counterclockwise when looking at the light from behind, facing its direction of propagation. In studying Figure 9 it becomes evident that if the analyser polarizer needed to be rotated clockwise to block the light again, then the crystal rotated it in an overall clockwise fashion as well. Thus, the group found the results written in Table 13 for the direction in which the birefringent crystals rotated the sample.

Crystal	Polarization Rotation
Crystal 1	$30° \pm 10°$ clockwise
Crystal 2	$60° \pm 10°$ clockwise
Crystal L	$25° \pm 10°$ counterclockwise

Table 13: Rotation of Polarization of Light by Birefringent Crystals

5 Discussion

5.1 Beam Propagation, Law of Reflection, and Snellius Law Experiment

Compared with expected result, our measured value of refractive index of Plexiglas , $n_{glass} = 1.50$, with a deviation of 0.02, is very close to the expected result of 1.489.(6). The refractive index of Plexiglas calculated from the total internal reflection of Plexiglas is $n_{glass} = 1.506$, which also suggests proper measurement scheme. The refractive index of the Plexiglas calculated from the Brewster angel is $n = 1.2774$, which is due to the experiment setup, where the position of the laser source is not stable enough to make steady measurement.

Our measurement value of refractive index of water , $n_{gamma} = 1.24 \pm 0.09$, is also close to the expected value of $n = 1.33$. The slight error might result from difficulty of observing the laser beam light in water.

Our measurement values of the parallel shift of the Plexiglas is also very close to the expected values calculated theoretically. However, our measurement result of the refractive index of the Plexiglas from Brewster angel measurement deviates from the expected value in a large extend. This might due

To improve the accuracy of our measurement, we could further decrease the spot size of the laser to decrease the uncertainty produced by direct observational measurement. Further experiments would need to be made with the equipment used to determine the source of this systematic error.

5.2 Prism Dispersion

Without knowing the type of glass that the prism was made of, it is impossible to determine the theoretical values of the prism dispersion and prism refractive index. It is also impossible to determine the error of the measured results.

The method used to gauge whether the beam was passing through the prism parallel to the beam base was the main source of error. Using only a slip of paper and comparing the endpoints of the path passing through the prism with the naked eye is very prone to human error. This method also made it close to impossible to gauge the size of the uncertainty in the angle. In future experiments, a better method for visualizing the beam's passage within the prism should be used. One possibility is to make two etchings or engravings in the sides of the prism that the beam passes through. The engravings will scatter a portion of the laser light when the beam passes through them, enabling the human eye to see whether the laser is passing through the engraving or not. If the engravings are made equal distances along their respective sides from the base, then if scattering from both engravings is detected, the beam is passing a line parallel to the base. For an accurate uncertainty determination, fabrication tolerances will have to be evaluated and included. More uncertainty will result from the radius and circularity of the beam. Implementing the etchings or another solution would increase both the repeatability and reproducibility of the measurements.

5.3 Diffraction

Without knowing the spacing of the slits in the grating, it is impossible to determine the theoretical value of the grating dispersion and thus the error of the measured results.

The main issue with this experiment was its susceptibility to human error in reading the angle. The protractor to gauge the angle was below the beam, and as described in Section 3.4, the operator of the experiment needed to improvise a semicircular screen. The method chosen, to bend a piece of paper by hand, was largely prone to error. The group did not succeed in improvising a truly semicircular screen. This also affected the ability to gauge the uncertainty of the measurement. In future experiments, one possibility to improve the measurement's accuracy and reduce the uncertainty would be to fabricate a semicircular screen with a known radius of curvature and protractor lines drawn

vertically onto it spaced .5° apart would facilitate better measurements. The radius of curvature would determine the distance that the screen's center should be placed from the edge of the diffraction grating facing away from the incident beam. The uncertainty would be minimized to at least the .5° stemming from the scale used in the protractor and the size and shape of the beam. Implementing this solution would increase both the repeatability and reproducibility of the measurements and isolate the uncertainty as stemming from the laser spot size.

5.4 Rotation of Polarization by Birefringent Crystals

Without knowing what type of birefringent crystals were used, it is impossible to determine the error in the measured angles. One difficulty in taking the measurements was that the beam never truly disappeared. Instead, even if the brightness was observed to decrease to a level seeming close to zero, within a second a small bright spot appeared again. This leads to the conclusion that the incoming light's polarization was not constant. This may be due to the laser light interacting dynamically with the birefringent crystal, or the polarizers not working as intended. Further experiments would need to be made with the equipment used to determine the source of this systematic error.

6 Conclusion

This set of experiments was aimed at studying Snell's laws of reflection and refraction, total internal reflection, parallel shift in a rectangular piece of glass, the dispersion of light within a triangular prism, the diffraction of light by a grating, and the rotation of light's linear polarization by a birefringent crystal. While the results agreed roughly with the expected outcome, there were large uncertainties due to the equipment used. Improvement and tuning of the equipment can decrease the uncertainty and improve the accuracy, precision, reproducibility and repeatability of the measurements in future experiments.

7 References

References

[1] https://en.wikipedia.org/wiki/Fresnelequations/media/File:Fresnel1.svg *Variables used in the Fresnel equations.* Wikipedia Contributors, 28 December 2018.

[2] https://commons.wikimedia.org/wiki/File:SingleSlitDiffraction.svg *Single Slit Diffraction.* jkrieger, 14 March 2012.

[3] http://farside.ph.utexas.edu/teaching/302l/lectures/node127.html *Law of Reflection.* Richard Fitzpatrick, 2007.

[4] https://www.asp.uni-jena.de/aspmedia/Optics+Training+Laboratory/Setup+Descriptions/SetupFundamentals.pdf *Laboratory Handout.* Abbe School of Photonics, January 2019

[5] https://www.britannica.com/science/refractive-index *Refractive Index.* The Editors of Encyclopaedia Britannica, 28 December 2018

[6] https://www.filmetrics.com/refractive-index-database/Acrylic/Acrylate-Lucite-Perspex-Plexiglas *Plexiglas Refractive Index* FILMETRICS January 2019